Carbon-Nitrogen bond formation on Cu electrodes during CO_2 reduction in NO_3^- solution

Piotr Krzywda
University of Twente https://orcid.org/0000-0002-8265-5080
Ainoa Paradelo Rodríguez
University of Twente
Nieck Benes
University of Twente
Bastian Mei
University of Twente https://orcid.org/0000-0002-3973-9254
Guido Mul (G.mul@utwente.nl)
University of Twente

Article

Keywords: CO2 reduction, Cu electrodes, carbon-nitrogen bonds

Posted Date: September 9th, 2021

DOI: https://doi.org/10.21203/rs.3.rs-841663/v1

Abstract

In performing electrochemical reduction of CO_2 over Cu electrodes, the anions present in solution typically do not participate in the formation of reaction products. NO_3^- is an exception, and previous reports indicate the formation of urea in certain process conditions. Here we demonstrate by use of Surface Enhanced Raman Spectroscopy and Electrochemical Mass spectrometry that simultaneous reduction of NO_3^- and CO_2 on Cu surfaces forms carbon-nitrogen bonds in the form of cyanide. The Raman peak position of C≡N is dependent on the oxidation state of the Cu surface, and Cu-C≡N can be oxidized by anodic polarization yielding NO. More importantly, Cyanide likely forms soluble Cu-C≡N complexes, which cause catalyst surface instability. The implications of this observation for practical application of a process for electrochemical formation of urea, are discussed.

Main Text

Urea is one of the most important nitrogen-based fertilizers playing a very important role in securing the worldwide food supply[1]. The chemical is industrially produced from CO_2 and NH_3 in an energy intensive process consuming 173 kWh per ton of urea[2], with an annual production capacity of 155 Mt[3]. Although ammonia needed for urea production is mainly produced by the Haber-Bosch process, non-conventional renewable technologies for ammonia synthesis, which can allow for small scale, green ammonia production, are gaining significant attention[4,5]. Unfortunately, while economically attractive, electrochemical N_2 reduction to NH_3 suffers from very low activity[6]. Alternatively, NO_3^- can be considered as feedstock, which provides facile reaction kinetics and requires a significantly lower overpotential[7–9]. Green ammonia from NO_3^- could be coupled with urea production in a consecutive reactor, located where waste NO_3^- streams are available[10].

Rather than application of an electrochemical- and catalytic reactor in series, proof of principle for simultaneous reduction of CO_2 and NO_3^- in a single electrochemical reactor, using gas diffusion electrodes, was established,[11–14] including the use of different nitrogen sources such as NO_3^- [15–17], NO_2^- [18–20] and N_2 [21–23]. Since copper is a good catalyst for CO_2 activation[24] as well as for NH_3 formation from NO_3^- [25], copper was mostly investigated for electrochemical urea synthesis. Usually anions present in solution do not participate in electrochemical transformation of CO_2 over Cu electrodes, but apparently NO_3^- is an exception. However, little is known about the C-N coupling mechanism on Cu surfaces, and the hypothesis in the literature of CO and NH_x surface intermediates is rather speculative. In the present study, we discuss the use of Surface Enhanced Raman Spectroscopy (SERS) to identify adsorbed species on a polycrystalline, rough Cu electrodes during simultaneous reduction of CO_2 and NO_3^-. SERS is a suitable technique to detect reaction intermediates and it was already used to monitor electrochemical reduction of CO_2 on Cu surfaces[26,27]. Moreover, Electrochemical Mass Spectrometry (EC-MS) was used to study potential dependent desorption of products from the electrode surface, which in combination with

SERS resulted in detailed understanding of the surface processes occurring during electrochemical reduction of CO_2 in the presence of NO_3^-. Formation of carbon-nitrogen bonds in the form of cyanide was revealed, which was never previously observed at room temperature in aqueous electrolyte.[28] We thus contribute to understanding of electrochemical C-N coupling reactions recently studied in the literature[29–32]. More importantly, we demonstrate that cyanide likely leads to formation of soluble Cu-C≡N complexes, which suggests a stable process for urea formation based on Cu electrodes might be difficult to achieve.

Results And Discussion

In situ **SERS of Cu electrode in the presence of CO_2 and NO_3^-**

SERS of the Cu surface in CO_2 saturated 0.1 M $KHCO_3$ with 50 mM KNO_3 during cyclic voltammetry was performed, and is shown separately for reductive and oxidative scans (Fig. 1b and 1c, respectively). The expected characteristic signals for Cu-oxides were observed in voltametry. In the reductive scan at 0.5 V reduction of CuO to Cu_2O is observed, followed by reduction of Cu_2O to metallic Cu (Fig. 1a). Those surface chemical changes are in agreement with alterations in intensity of the characteristic peaks at 610 and 520 cm^{-1} in the SER spectra, which have been assigned to Cu_2O[33] (Fig. 1b). At more negative potentials those signals disappear, only to re-appear again in an oxidative scan at 0.5 V (Fig. 1c) and higher, in agreement with the oxidative current in Fig. 1a, which can thus be assigned to oxidation of Cu to Cu_2O. Cyclic voltammograms of blank measurements can be found in the Supplementary Figure S1, and Raman spectra in reference conditions in Supplementary Figures S2 (CO_2 reduction in bicarbonate solution) and S3 (nitrate reduction in the absence of CO_2), confirming that the Raman peaks at 1048 and 1072 cm^{-1} in Figs. 1b and 1c can be assigned to nitrate in solution, and surface adsorbed carbonate, respectively.

In a reductive scan (Fig. 1b) up to 0.3 V, little changes are observed in the Raman spectra. When reduction of Cu-oxides is completed, a signal at ~ 2080 cm^{-1} appears and grows in intensity at more negative potential. Although the band position is similar to that assigned to adsorbed C ≡ O, the potential at which this band is observed (0.3 V vs RHE) is quite different from previous observations in the absence of nitrate. Moreover, the standard reduction potential of CO_2 to CO is -0.106 V *vs* RHE[34], and since the first CV cycle is shown excluding residual CO from previous scans, CO cannot be present at 0.3 V vs RHE. At more negative potentials (-0.7 V vs RHE), the signal at 360 cm^{-1} from Cu-CO should appear in case CO is actually formed (Supplementary Figures S2 and S4). However, such signal is not observed at any moment during a CV in the presence of NO_3^-. In addition, the CO signal at 2080 cm^{-1} observed in the absence of nitrate has relatively low intensity compared to the peak observed here (Magnification in Fig. 1b). Surprisingly, although the intensity of adsorbed CO_3^{2-} at 1070 cm^{-1} decreases at more negative potential, it doesn't disappear completely, and appears more stable in the presence, than in the absence of nitrate (compare the measurement in the absence of nitrate in Supplementary Figure S4). This could

suggest that the presence of NO_3^- in the system prevents conversion of surface adsorbed CO_2 to CO to some extent, which is in agreement with the absence of signals of CO in the Raman spectra. The presence of small amounts of NO_x in CO_2 has been previously found to significantly reduce selectivity of CO_2RR (favouring nitrate reduction products), because of the lower onset potential for reduction of NO_x compared to CO_2[34,35].

During the oxidative scan (Fig. 1c), the 2080 cm^{-1} peak does not disappear at -0.4 V vs RHE like in the case of CO formed by reduction of CO_2. This is additional proof that the observed signal originates from a product formed only in the presence of NO_3^- and CO_3^{2-}. Finally, when Cu_2O is formed (0.5 V vs RHE), the ~ 2080 cm^{-1} peak disappears while a new signal at 2150 cm^{-1} appears. The Stark effect (Supplementary Figure S5), proving that the signals originate from surface-absorbed species, is observed for both the ~ 2080 cm^{-1} and 2150 cm^{-1} bands, respectively. Besides CO, carbon-nitrogen triple bonds (C ≡ N) show significant intensity in the wavenumber range of interest, out of which cyanide is the most simple compound[43,44]. Although it was also reported that Cu-H (adsorbed hydrogen) can appear at the same position in SEIRAS[45], in a control experiment in Ar saturated 0.1 M $KClO_4$ signals were absent (Supplementary Figure S6).

In order to prove that the reaction is electrochemically driven, SERS of a Cu surface in CO_2 saturated 0.1 M $KHCO_3$ with 50 mM KNO_3 was recorded at OCV (Fig. 2a). Clearly bands in the 2000–2500 cm^{-1} remain absent as a function of time. At -0.3 V vs RHE, a broad peak at 2080 cm^{-1} appears and remains visible throughout the measurement. Subsequently, at OCV when Cu_2O signals re-appear due to surface oxidation of metallic Cu, the band at 2150 cm^{-1} appears and slightly decreases in intensity over time while shifting position from 2154 cm^{-1} to 2149 cm^{-1}. This suggests that the product formed under reductive potential, changes frequency when oxidation of Cu occurs to form a Cu_2O containing surface. Moreover, in order to exclude any homogeneous reactions induced by possible Cu ions present in the solution, cyclic voltammetry in blank electrolytes was performed and SERS at OCV was measured while adding $KHCO_3$ or KNO_3 (Fig. 2b). The signal at 2150 cm^{-1} was not observed in any experiment, proving that the reaction is driven electrochemically and can be assigned to CuC ≡ N.

A summary of the observed SERS signals can be found in Table 1.

Table 1
Summary of SERS signals observed in this work. *Signals related to cyanide observed in this work.

Position [cm^{-1}]	Assignment	Ref.
275	Cu-CO	27,36
360		
350	CO_3^{2-} $(C\text{-}O)_{asym}$	27
1540		
520	Cu_2O	33
610		
1048	NO_3^-	37,38
1072	CO_3^{2-} $(C\text{-}O)_{sym}$	27,39
1360	bicarbonate	27
1640	H_2O	27
2070	$C \equiv O$	27,39
~ 2080*	$Cu(C \equiv N)_n^{(n-1)}$	40,41
~ 2150*	$CuC \equiv N$	40
300*	Cu-CN	42

We will now discuss if $C \equiv N$ is a possible product of reduction of urea, or formed in a route via intermediates.

Urea decomposition – Does it form Cu-CN?

Surprisingly, the bands observed in the Raman spectra of Fig. 2, do not provide much information regarding (intermediates in) the formation of urea. To evaluate urea chemistry over Cu surfaces, potential dependent SERS analysis of 50 mM urea, in CO_2 saturated 0.1 M $KHCO_3$, is shown in Supplementary Figure S7. Several Raman signals can be assigned to adsorbed urea on Cu surfaces, while a strong vibration at 713 cm^{-1} is apparent after reduction of Cu_2O at 0 V vs RHE (Figure S7a), shifting to lower frequency as a function of increasingly negative potential (Figures S7b and S7c). We speculate this band is due to the C-N vibration (strong at ~ 1005 cm^{-1} in solution) of urea, shifted to lower wavenumber by strong adsorption/interaction of urea with the Cu/Cu^+ surface. Interestingly, when urea is exposed to Cu

at reductive potentials, a Cu-C ≡ N related signal appears in the Raman spectra, as well as the Cu-CO band at ~ 360 cm^{-1} at the most negative potentials (< -0.9 V) applied, the result of conversion of CO_2 to CO and coinciding with the disappearance of the peak at ~ 710 cm^{-1}. Apparently urea does not prevent reduction of CO_2, contrary to nitrate.

Urea in solution can undergo multiple reactions, but formation of C ≡ N has not been previously reported in reductive conditions[46,47]. It can hydrolyse to cyanate and ammonium, which is a reversible reaction[48]. In neutral solution, cyanate may decompose further to produce ammonium ions and carbonate [49]. Is should be noted that urea was not formed by reaction of ammonium carbonate solution, suggesting that consecutive cyanate decomposition renders urea decomposition irreversible[50]. Reduction of cyanate to C ≡ N appears feasible, but was not experimentally proven.

Cu-CN: intermediate to Urea?

Also the role of C ≡ N in the electrochemical path towards urea, if any is formed from CO_2 and NO_3^-, remains difficult to assess on the basis of the Raman experiments. Since the characteristic Raman feature at ~ 709 cm^{-1} related to urea adsorption is completely absent in Figs. 1b and 1c, C ≡ N is most likely formed by conversion of a short lived (common) intermediate, such as a C-N species.

In order to prove that the observed signals belong to cyanide, and evaluate potential consecutive reactions of C ≡ N, SERS of the Cu surface in CO_2 saturated $KHCO_3$ in the presence of KCN was measured as shown in Fig. 3.

In the presence of 10 ppb of KCN, a signal at 2147 cm^{-1} appears (Fig. 3a) which matches the peak observed in our experiments. It was proven that SERS can be successfully used for detection of trace amounts of cyanides as demonstrated for Au in the gas phase[42] as well as in solution on Ag[51] and Cu surfaces, where Cu(I) surfaces can be very effective in detection by forming CuCN[52]. The position of the peak is similar to the C ≡ N stretching position (frequency) of solid CuCN[40] and surprisingly, it changes depending on CN^- concentration (Fig. 3b). In excess of CN^- in aqueous solution, CuCN can form higher, soluble complexes, generalized as $Cu(CN)_n^{(n-1)}$ (n = 2, 3, 4), which structure depends on the CN^-/Cu ratio[53]. At higher CN^- concentration, the Raman signals of Cu_2O decrease in intensity (Supplementary Figure S8), which proves chemical reaction of CN^- to be likely with (surface) copper oxide, forming higher CuCN-complexes[54].

In order to verify the behaviour of the C ≡ N signal during a potential sweep, cyclic voltammetry in 0.1 M $KHCO_3$ with addition of 0.1 ppm of KCN was performed (Fig. 4). The obtained results, i.e. strong signals at ~ 2080 cm^{-1}, are in excellent agreement with the experimental results obtained in CO_2 and NO_3^- containing electrolyte. Note that NO_3^- was not added in this measurement, thus those signals must originate from C ≡ N. $Cu(CN)_n^{(n-1)}$ can give different Raman signals depending on the type of complex and usually more than one is present in the system, which can depend on the concentration of CN^- as

well as the pH of the solution[40,41]. In our system, considering continuous production of CN^- at negative potentials in a CV cycle as well as a pH change near the electrode surface it is reasonable to assign the set of ~ 2080 cm^{-1} peaks to $Cu(CN)_n^{(n-1)}$. Formation of HCN is also possible considering the bulk pH of the electrolyte being 8.6, although this is much more favourable at lower pH[41].

If higher KCN concentrations were used (Supplementary Figure S9), Cu_2O signals were hardly recorded during a CV, which again confirms chemical attack of CN^- on Cu(I)-oxide forming Cu-CN complexes. This likely explains the broad peak observed even at positive potentials, and the very small signal at 2170 cm^{-1} attributed to CuCN.

Finally, in order to definitively prove formation of cyanide, isotopic labelling experiments with $KH^{13}CO_3$ and $K^{15}NO_3$ were performed (Supplementary Figure S10). The results show peak shifts with both, ^{13}C and ^{15}N, proving involvement of carbon and nitrogen in the species responsible for the observed vibrations at ~ 2080 and ~ 2150 cm^{-1}.

Consequences of Cu-C ≡ N formation

The electrode surface was analysed after chronoamperometry at -0.3 V vs RHE. The electrochemical surface area was significantly increased indicating surface roughening, and the XRD pattern shows a specific increase of the Cu (220) orientation (Supplementary Figure S11). Moreover, on SEM images surface changes can be observed (Supplementary Figure S12). These results all indicate surface reorganization occurs by C ≡ N formation, and thus surface instability during electrolysis in the presence of CO_2 and NO_3^- is likely. This might have significant consequences for a practical process for formation of urea, but this requires further study.

Reactions of formate and NH_4^+

In order to reveal what intermediate species might be responsible for reaction towards cyanide, cyclic voltammetry with formate instead of bicarbonate and ammonium salt instead of nitrate were performed (Supplementary Figure S13 and S14). Since at 0.3 V no CO_2 reduction products are expected (see standard reduction potentials of CO_2 in Supplementary Table S1), formate was chosen as one of the most simple products from CO_2 reduction in a $2e^-$ transfer[55]. On the other hand, NH_4^+ was chosen as N-source, since this is the most likely product of NO_3^- reduction on Cu surfaces[56]. In both cases, no signals related to cyanide were observed.

Since cyanide formation requires removal of oxygen from NO_3^-, it is very likely that NH_x intermediates on the electrode surface are involved in the reaction (it was reported that stable NH_x adsorbed on cathode surface can exist[57]). Furthermore, adsorbed carbonate is present in the potential range where adsorbed NH_x species exist. Therefore, we conclude that adsorbed NH_x on Cu surface reacts with adsorbed CO_3^{2-} forming cyanide and water, as shown in the schematic overview in Fig. 6.

In situ **EC-MS analysis**

In order to complement the results obtained by SERS, electrochemical mass spectrometry was used which allows to track gaseous products desorbed from the electrode surface with high sensitivity[58]. Mass spectra of selected signals recorded during CV scans are shown in Supplementary Figure S15, Figure S16 and Figure S17. Comparison of the m/z: 30 signal, in different electrolytes is shown in Fig. 5a. Besides the obvious difference in m/z: 30 signal, assigned to NO, no other differences were observed. Formation of nitric oxide was confirmed by isotopically labelling experiments, where the peak of m/z: 31 is clearly visible when $K^{15}NO_3$ was used (Supplementary Figure S18).

In CO_2 saturated $KHCO_3$ with 50 mM KNO_3 as well as in Ar saturated 0.1 M KNO_3, NO is observed in the reductive sweep as product of NO_3^- electroreduction (NO was not found in CO_2 saturated $KHCO_3$). The difference in onset potential for NO formation can be explained by different concentrations of NO_3^- or pH changes in the electrolyte. Although the starting pH is the same (6.8), in the case of CO_2 saturated $KHCO_3$ the buffering capacity of the electrolyte renders large pH changes less likely as compared to electrolytes containing KNO_3 only. It could also very well be that residual C ≡ N species and adsorbed carbonate inhibit the reduction of NO_3^- somewhat, further explaining the different trend in NO production as a function of potential. More importantly, nitric oxide is also observed in an oxidative scan if CO_2 and NO_3^- are present. It starts to appear at ~ 0.4 V which matches the onset potential of the formation of the peak at 2150 cm^{-1} in SERS experiments. In addition, nitric oxide formation was monitored during chronoamperometry at -0.3 V vs RHE where no signal was detected as shown in Fig. 5b. However, when approaching OCV conditions, the NO signal appears and slowly decreases over time again, which is in agreement with the SERS spectra recorded at OCV (see Fig. 2; blank measurement with 0.1 M KNO_3 can be found in Supplementary Figure S19).

The formation of NO during an oxidative scan suggests oxidation of a (surface adsorbed) product, formed in the reductive scan, which based on SERS data is cyanide. Formed cyanide in solution can thus be decomposed by direct electrooxidation[59]. Cu is effective in this reaction by forming complexes which can oxidize at less positive potentials than free cyanide. It has been previously shown that those complexes can be oxidized at potentials slightly more positive than 0 V vs RHE[60]. Although the most desired products of oxidation of CN are N_2 and CO_2; OCN^-, CO_3^{2-}, NO_3^- and NH_3 were also observed[46]. Moreover, oxidation to NO_3^- was found to be catalysed by copper oxide[61] which very likely involves NO as intermediate. In our analysis system, NO starts to show up at 0.4 V where oxidation of cyanide complexes is possible on Cu electrodes, and the peak of this signal is observed at potentials where copper is oxidized, which is in agreement with literature.

The overall mechanism deduced from SERS and EC-MS experiments is schematically shown in Fig. 6, representing one cyclic voltammetry cycle. This scheme will be discussed in the following summary.

Summary

Simultaneous electroreduction of CO_2 and NO_3^- on Cu electrodes was investigated using Surface Enhanced Raman Spectroscopy and Mass Spectrometry. Initially reduction of nitrate results in the formation of NO. At less positive potentials very likely surface bound NH_x are formed, which react with adsorbed carbonate to Cu containing C ≡ N complexes. Evidence for formation of urea was not found. Reversing the scan to more positive potentials, likely results in deposition of solid CuCN and at the same time nitric oxide formation from oxidation of cyanide complexes was detected. These results reveal a novel reaction scheme in the simultaneous reduction of CO_2 and NO_3^-. Furthermore the results show the formation of other carbon-nitrogen species should be taken into account when working on electrochemical urea synthesis. Similarly, Cu instability due to chemical attack of CN^- as well as formation of toxic cyanides should be considered as potential difficulties in bulk electrolysis experiments with Cu. In addition we here provide important insights into research on C-N coupling reactions. Finally, the in situ formed cyanide might be coupled to organic molecules, and be a novel route towards industrially relevant cyanides or nitriles.

Methods

Materials

Cu foil (Alpha Aesar, 99.99%), or Cu disc (Pine research) and H_3PO_4 (Sigma Aldrich, 85 wt. % in H_2O,) were used for electrode preparation. Electrolyte solutions were prepared using MiliQ water and $KClO_4$ (Sigma Aldrich, 99.99 %), $KHCO_3$ (Sigma Aldrich, 99.7 %), KNO_3 (Sigma Aldrich, ≥ 99.0 %), $(NH_4)_2CO_3$ (Sigma Aldrich, ≥ 99.5 %), HCOOK (Sigma Aldrich, ≥ 99.0 %), KCN (Sigma Aldrich, ≥ 98.0 %), $K^{15}NO_3$ (Sigma Aldrich, 98 atom % ^{15}N), $KH^{13}CO_3$ (Sigma Aldrich, 99 atom% ^{13}C), $^{13}CO_2$ (Campro Scientific, min. 99.9 atom % ^{13}C).

Electrode preparation

For SERS experiments, polycrystalline rough Cu electrodes were prepared according to the procedure described elsewhere[27]. In brief, Cu discs were mechanically polished followed by anodic treatment in 85% phosphoric acid (3 V for 2.5 min), sonication in MiliQ water and drying in an Ar stream. A photograph of the prepared electrode is shown in Supplementary Figure S20.

For EC-MS experiments a Cu disc (⌀ 5 mm) was polished following the routine of cleaning provided by Pine Research.

Characterization

Electrodes were characterized using X-ray diffraction (XRD, Bruker Phaser D2) and Scanning Electron Microscopy (SEM) (JSM-6010LA, JEOL system).

Electrochemical measurements

Raman spectra were recorded using an Avantes AvaRaman spectrometer equipped with an Intertec λ = 785 nm laser. The distance between the Raman probe with a focal length of 10mm and the Cu surface was adjusted as to obtain the largest intensity of Raman signals. Electrolyte flow was adjusted to 1.8 ml/min. Ag/AgCl (3 M NaCl, BASi) and platinized Ti mesh were used as reference and counter electrode respectively. The schematic representation of the cell design is shown in Supplementary Figure S21. Each electrode was electrochemically activated *in situ* in 0.1 M $KClO_4$ by 5 oxidation-reduction cycles in the range between 2 and − 1.4 V vs RHE (SEM of Cu electrode before and after activation is shown in Supplementary Figure S22). Next, the electrolyte was changed for compositions reflecting the process conditions of urea formation or respective blanks. The electrolyte was continuously purged with CO_2 or Ar. Raman spectra were recorded during cyclic voltammetry (unless indicated otherwise) between + 0.9 and − 1.1 V vs RHE starting at the oxidative potential with a scan speed of 10 mV/s and spectral integration time of 5 s. The potential interval between spectra in the presented graphs is 0.2 V, unless otherwise indicated.

Chronoamperometry measurements were performed in a one compartment cell, with Ag/AgCl (3 M NaCl, BASi) and platinized Ti mesh used as reference and counter electrode respectively. The electrolyte was continuously purged with CO_2 or Ar. A potential of -0.3 V vs RHE was applied for 30 min. The Cu electrode was removed from the electrolyte immediately after the open-circuit potential was applied. Then it was rinsed with MiliQ water and dried in an Ar stream. The electrochemical surface area (ECSA) was measured before and after chronoamperometry by the capacitance method. Cyclic voltammograms in the potential region where no faradaic current is observed, were measured at variable scan rates from 20 to 100 mV/s in Ar saturated 0.1 M $KClO_4$.

EC-MS measurements were performed using a SpectroInlets (Copenhagen, Denmark) system, with He or CO_2 as carrier gas at 1 ml/min flow rate. Different m/z signals were recorded during cyclic voltammetry (unless otherwise indicated). Ag/AgCl (sat. KCl, CH Instrument) and Pt mesh were used as reference and counter electrode respectively. The schematic representation of the cell design is shown in Supplementary Figure S21.

All electrochemical measurements were carried out at room temperature using a BioLogic VSP potentiostat. Recorded potentials were recalculated to Reversible Hydrogen Electrode scale according to following equation:

$$E_{RHE} = E_{Ag/AgCl} + 0.059pH + E^0_{Ag/AgCl}$$

Declarations

Acknowledgements

This work took place within the framework of the Institute of Sustainable Process Technology, co-funded with subsidy from the Topsector Energy by the Ministry of Economic Affairs and Climate Policy, The Netherlands.

Author contributions

P. M. K. performed experiments, analysed the data and wrote the manuscript. A. P. R. performed EC-MS measurements. B. T. M., N. E. B. and G. M. supervised the work. All authors discussed the results and assisted during manuscript preparation.

Competing interests

The authors declare no competing interests.

Additional information

Supplementary information is available for this paper at LINK.

The authors declare that the data supporting the findings of this study are available within the paper and its Supplementary Information files.

Correspondence and requests for materials should be addressed to G.M.

References

1. Meessen, J. H. Urea. *Ullman's Encyclopedia of Industrial Chemistry* 657–695 (2012).
2. Fiamelda, L., Suprihatin & Purwoko. Analysis of water and electricity consumption of urea fertilizer industry: Case study PT. X. *IOP Conf. Ser. Earth Environ. Sci.* **472**, (2020).
3. Aresta, M., Dibenedetto, A. & Angelini, A. Catalysis for the valorization of exhaust carbon: From CO2 to chemicals, materials, and fuels. technological use of CO2. *Chem. Rev.* **114**, 1709–1742 (2014).
4. Rouwenhorst, K. H. R., Krzywda, P. M., Benes, N. E., Mul, G. & Lefferts, L. Ammonia, 4. Green Ammonia Production. *Ullmann's Encyclopedia of Industrial Chemistry* 1–20 (2020).
5. Rouwenhorst, K. H. R., Krzywda, P. M., Benes, N. E., Mul, G. & Lefferts, L. Ammonia Production Technologies. in *Techno-Economic Challenges of Green Ammonia as an Energy Vector* 41–83 (2020).
6. Andersen, S. Z. *et al.* A rigorous electrochemical ammonia synthesis protocol with quantitative isotope measurements. *Nature* **570**, 504–508 (2019).
7. Hao, D. *et al.* Emerging alternative for artificial ammonia synthesis through catalytic nitrate reduction. *J. Mater. Sci. Technol.* **77**, 163–168 (2021).
8. Katsounaros, I. On the assessment of electrocatalysts for nitrate reduction. *Curr. Opin. Electrochem.* **28**, 100721 (2021).

9. McEnaney, J. M. *et al.* Electrolyte Engineering for Efficient Electrochemical Nitrate Reduction to Ammonia on a Titanium Electrode. *ACS Sustain. Chem. Eng.* **8**, 2672–2681 (2020).
10. Greenlee, L. F. Recycling fertilizer. *Nat. Energy* **5**, 557–558 (2020).
11. Shibata, M., Yoshida, K. & Furuya, N. Electrochemical synthesis of urea on reduction of carbon dioxide with nitrate and nitrite ions using Cu-loaded gas-diffusion electrode. *J. Electroanal. Chem.* **387**, 143–145 (1995).
12. Shibata, M., Yoshida, K. & Furuya, N. Electrochemical synthesis of urea at gas-diffusion electrodes Part II. Simultaneous reduction of carbon dioxide and nitrite ions at Cu, Ag and Au catalysts. *J. Electroanal. Chem.* **442**, 67–72 (1998).
13. Shibata, M., Yoshida, K. & Furuya, N. Electrochemical Synthesis of Urea at Gas-Diffusion Electrodes III. Simultaneous Reduction of Carbon Dioxide and Nifrite Ions with Various Metal Catalysts. *J. Electrochem. Soc.* **145**, 595 (1998).
14. Shibata, M., Yoshida, K. & Furuya, N. Eleetroehemical Synthesis of Urea at Gas dliffusion Eleetrodes V. Simultaneous Reduction of Carbon Dioxide and Nitrite Ions with Various Boride Catalysts. *Denki Kagaku* **6**, 584 (1998).
15. Saravanakumar, D., Song, J., Lee, S., Hur, N. H. & Shin, W. Electrocatalytic Conversion of Carbon Dioxide and Nitrate Ions to Urea by a Titania–Nafion Composite Electrode. *ChemSusChem* **10**, 3999–4003 (2017).
16. Siva, P., Prabu, P., Selvam, M., Karthik, S. & Rajendran, V. Electrocatalytic conversion of carbon dioxide to urea on nano-FeTiO3. *Ionics (Kiel).* **23**, 1871–1878 (2017).
17. Lv, C. *et al.* Selective electrocatalyic synthesis of urea with nitrate and carbon dioxide. *Nat. Sustain.* (2021) doi:10.1038/s41893-021-00741-3.
18. Meng, N. *et al.* Electrosynthesis of urea from nitrite and CO2 over oxygen vacancy-rich ZnO porous nanosheets. *Cell Reports Phys. Sci.* **2**, 100378 (2021).
19. Feng, Y. *et al.* Te-Doped Pd Nanocrystal for Electrochemical Urea Production by Efficiently Coupling Carbon Dioxide Reduction with Nitrite Reduction. *Nano Lett.* **20**, 8282–8289 (2020).
20. Cao, N. *et al.* Oxygen vacancies enhanced cooperative electrocatalytic reduction of carbon dioxide and nitrite ions to urea. *J. Colloid Interface Sci.* **577**, 109–114 (2020).
21. Chen, C. *et al.* Coupling N2 and CO2 in H2O to synthesize urea under ambient conditions. *Nat. Chem.* **12**, (2020).
22. Menglei Yuan *et al.* Unveiling Electrochemical Urea Synthesis by Co-Activation of CO2 and N2 with Mott-Schottky Heterostructure Catalysts. *Angew. Chemie - Int. Ed.* **60**, 10910–10918 (2021).
23. Yuan, M. *et al.* Electrochemical C-N coupling with perovskite hybrids toward efficient urea synthesis. *Chem. Sci.* **12**, 6048–6058 (2021).
24. Shah, A. H. *et al.* Revisiting Electrochemical Reduction of CO2 on Cu Electrode: Where Do We Stand about the Intermediates? *J. Phys. Chem. C* **122**, 18528–18536 (2018).

25. Rosca, V., Duca, M., DeGroot, M. T. & Koper, M. T. M. Nitrogen Cycle Electrocatalysis. *Chem. Rev.* **109**, 2209–2244 (2009).
26. Markin, A. V., Markina, N. E., Popp, J. & Cialla-May, D. Copper nanostructures for chemical analysis using surface-enhanced Raman spectroscopy. *rends Anal. Chem.* **108**, 247–259 (2018).
27. Moradzaman, M. & Mul, G. In Situ Raman Study of Potential-Dependent Surface Adsorbed Carbonate, CO, OH, and C Species on Cu Electrodes During Electrochemical Reduction of CO2. *ChemElectroChem* **8**, 1478–1485 (2021).
28. Tang, C., Zheng, Y., Jaroniec, M. & Qiao, S. Z. Electrocatalytic Refinery for Sustainable Production of Fuels and Chemicals. *Angew. Chemie - Int. Ed.* 2–21 (2021) doi:10.1002/anie.202101522.
29. Wu, Y., Jiang, Z., Lin, Z., Liang, Y. & Wang, H. Direct electrosynthesis of methylamine from carbon dioxide and nitrate. *Nat. Sustain.* (2021) doi:10.1038/s41893-021-00705-7.
30. Jouny, M. *et al.* Formation of carbon–nitrogen bonds in carbon monoxide electrolysis. *Nat. Chem.* **11**, 846–851 (2019).
31. Tao, Z. *et al.* Cascade electrocatalytic reduction of carbon dioxide and nitrate to ethylamine. *J. Energy Chem.* **65**, 367–370 (2022).
32. Kim, J. E. *et al.* Electrochemical Synthesis of Glycine from Oxalic acid and Nitrate. *Angew. Chemie Int. Ed.* (2021) doi:10.1002/anie.202108352.
33. Chan, H. Y. H., Takoudis, C. G. & Weaver, M. J. Oxide film formation and oxygen adsorption on copper in aqueous media as probed by surface-enhanced Raman spectroscopy. *J. Phys. Chem. B* **103**, 357–365 (1999).
34. Ko, B. H. *et al.* The impact of nitrogen oxides on electrochemical carbon dioxide reduction. *Nat. Commun.* **11**, 1–9 (2020).
35. Choi, B. U., Tan, Y. C., Song, H., Lee, K. B. & Oh, J. System Design Considerations for Enhancing Electroproduction of Formate from Simulated Flue Gas. *ACS Sustain. Chem. Eng.* **9**, 2348–2357 (2021).
36. Gunathunge, C. M. *et al.* Spectroscopic Observation of Reversible Surface Reconstruction of Copper Electrodes under CO2 Reduction. *J. Phys. Chem. C* **121**, 12337–12344 (2017).
37. Zhou, Z., Huang, G. G., Kato, T. & Ozaki, Y. Experimental parameters for the SERS of nitrate ion for label-free semi-quantitative detection of proteins and mechanism for proteins to form SERS hot sites: A SERS study. *J. Raman Spectrosc.* **42**, 1713–1721 (2011).
38. Mosier-Boss, P. A. & Lieberman, S. H. Detection of nitrate and sulfate anions by normal Raman spectroscopy and SERS of cationic-coated, silver substrates. *Appl. Spectrosc.* **54**, 1126–1135 (2000).
39. Chernyshova, I. V., Somasundaran, P. & Ponnurangam, S. On the origin of the elusive first intermediate of CO2 electroreduction. *Proc. Natl. Acad. Sci. U. S. A.* **115**, E9261–E9270 (2018).
40. Lukey, G. C., Van Deventer, J. S. J., Huntington, S. T., Chowdhury, R. L. & Shallcross, D. C. Raman study on the speciation of copper cyanide complexes in highly saline solutions. *Hydrometallurgy* **53**, 233–244 (1999).

41. Souza, C., Majuste, D. & Ciminelli, V. S. T. Effects of surface properties of activated carbon on the adsorption mechanism of copper cyanocomplexes. *Hydrometallurgy* **142**, 1–11 (2014).
42. Lauridsen, R. K. *et al.* Towards quantitative SERS detection of hydrogen cyanide at ppb level for human breath analysis. *Sens. Bio-Sensing Res.* **5**, 84–89 (2015).
43. Martín-Yerga, D. *et al.* Quantitative Raman spectroelectrochemistry using silver screen-printed electrodes. *Electrochim. Acta* **264**, 183–190 (2018).
44. Han, J., Blackburn, N. J. & Loehr, T. M. Identification of the Cyanide Stretching Frequency in the Cyano Derivative of Copper/Zinc-Superoxide Dismutase by Ir and Raman Spectroscopy. *Inorg. Chem.* **31**, 3223–3229 (1992).
45. Heyes, J., Dunwell, M. & Xu, B. CO2 Reduction on Cu at Low Overpotentials with Surface-Enhanced in Situ Spectroscopy. *J. Phys. Chem. C* **120**, 17334–17341 (2016).
46. Hwang, J. Y., Wang, Y. Y. & Wan, C. C. Electrolytic oxidation of cuprocyanide electroplating waste waters under different pH conditions. *J. Appl. Electrochem.* **17**, 684–694 (1987).
47. Woods, A. M. The Adsorption of Urea on Polycrystalline Gold Electrodes. (University of Saskatchewan, 2016).
48. Alexandrova, A. N. & Jorgensen, W. L. Why urea eliminates ammonia rather than hydrolyzes in aqueous solution. *J. Phys. Chem. B* **111**, 720–730 (2007).
49. Lister, M. W. Some Observations on Cyanic Acid and Cyanates. *Can. J. Chem.* **33**, 426–440 (1955).
50. Wen, N. & Brooker, M. H. Ammonium carbonate, ammonium bicarbonate, and ammonium carbamate equilibria: A raman study. *J. Phys. Chem.* **99**, 359–368 (1995).
51. Dao, T. C. *et al.* Modification of the SERS spectrum of cyanide traces due to complex formation between cyanide and silver. *Adv. Nat. Sci. Nanosci. Nanotechnol.* **9**, (2018).
52. Gopal Reddy, C. V., Yan, F., Zhang, Y. & Vo-Dinh, T. A highly sensitive Raman method for selective cyanide detection based on evaporated cuprous iodide substrate. *Anal. Methods* **2**, 458–460 (2010).
53. Valiuniene, A., Antanavičius, V., Margarian, Ž., Matulaitiene, I. & Valinčius, G. Electrochemical oxidation of cyanide using platinized Ti electrodes. *Medziagotyra* **19**, 385–389 (2013).
54. Wels, B. & Johnson, D. C. Electrocatalysis of Anodic Oxygen Transfer Reactions: Oxidation of Cyanide at Electrodeposited Copper Oxide Electrodes in Alkaline Media. *J. Electrochem. Soc.* **137**, 2785–2791 (1990).
55. Sun, Z., Ma, T., Tao, H., Fan, Q. & Han, B. Fundamentals and Challenges of Electrochemical CO2 Reduction Using Two-Dimensional Materials. *Chem* **3**, 560–587 (2017).
56. Tong, Z. *et al.* Nitrate reduction to ammonium: from CuO defect engineering to waste NOx-to-NH3 economic. *Energy Environ. Sci.* **14**, 3588–3598 (2021).
57. Duca, M., Cucarella, M. O., Rodriguez, P. & Koper, M. T. M. Direct reduction of nitrite to N2 on a Pt(100) electrode in alkaline media. *J. Am. Chem. Soc.* **132**, 18042–18044 (2010).
58. Trimarco, D. B. *et al.* Enabling real-time detection of electrochemical desorption phenomena with sub-monolayer sensitivity. *Electrochim. Acta* **268**, 520–530 (2018).

59. Dobrosz-Gómez, I., Gómez García, M. Á., Gaviria, G. H. & GilPavas, E. Mineralization of cyanide originating from gold leaching effluent using electro-oxidation: multi-objective optimization and kinetic study. *J. Appl. Electrochem.* **50**, 217–230 (2020).
60. Socha, A. & Kuśmierek, E. Electrochemical Oxidation of Cyanide Complexes with Copper at Carbon Fibre. in *Chemistry for the Protection of the Environment 2* 283–293 (Plenum Press, New York, 1996).
61. Cheng, S. C., Gattrell, M., Guena, T. & MacDougall, B. The electrochemical oxidation of alkaline copper cyanide solutions. *Electrochim. Acta* **47**, 3245–3256 (2002).

Figures

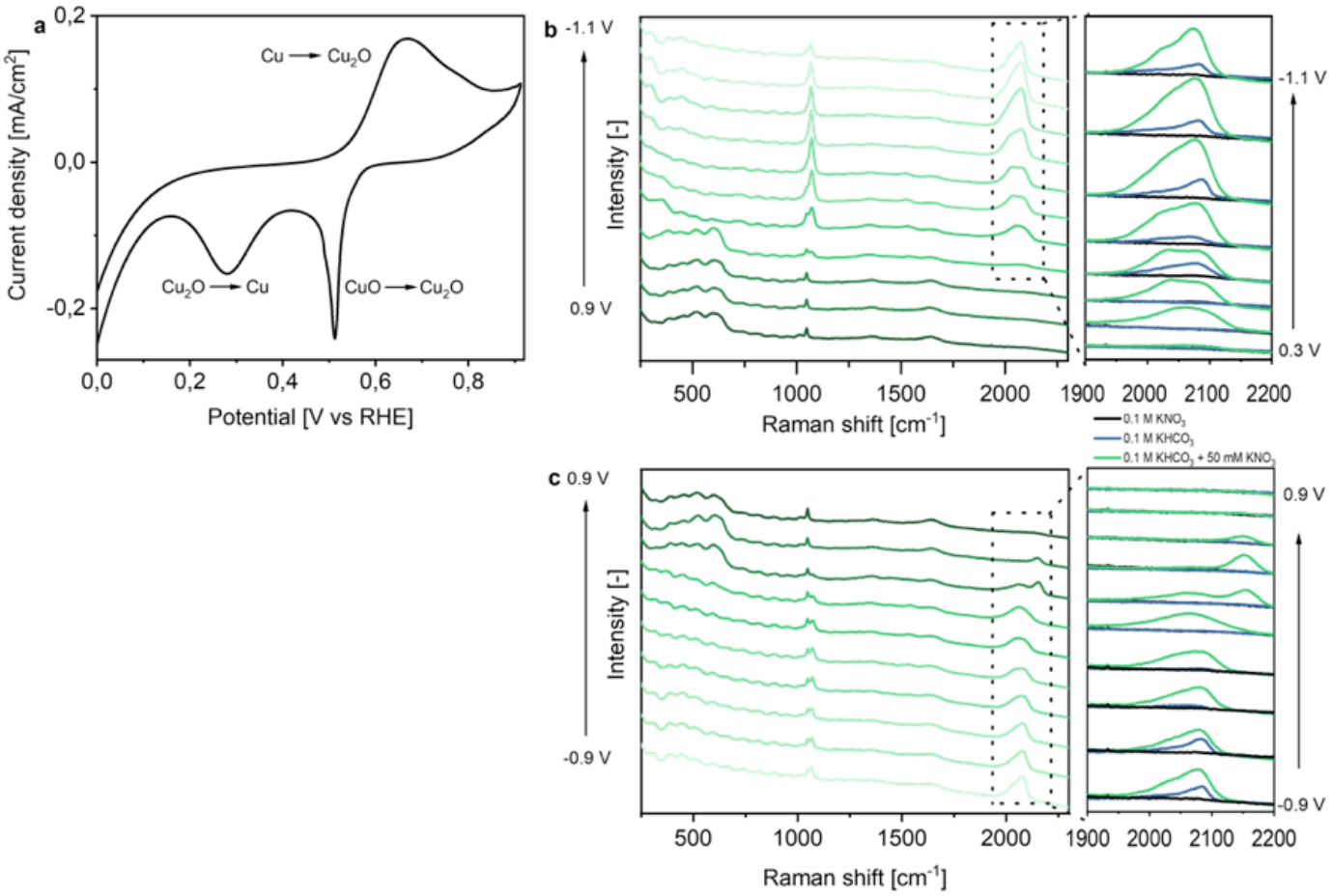

Figure 1

Cu catalyzed reduction of CO2 in saturated 0.1 M KHCO3 with 50 mM KNO3 electrolyte. (a) Cyclic voltammetry; (b) In situ SERS during a reductive scan and (c) during an oxidative scan, with magnification into the high wavelength region for the respective measurements.

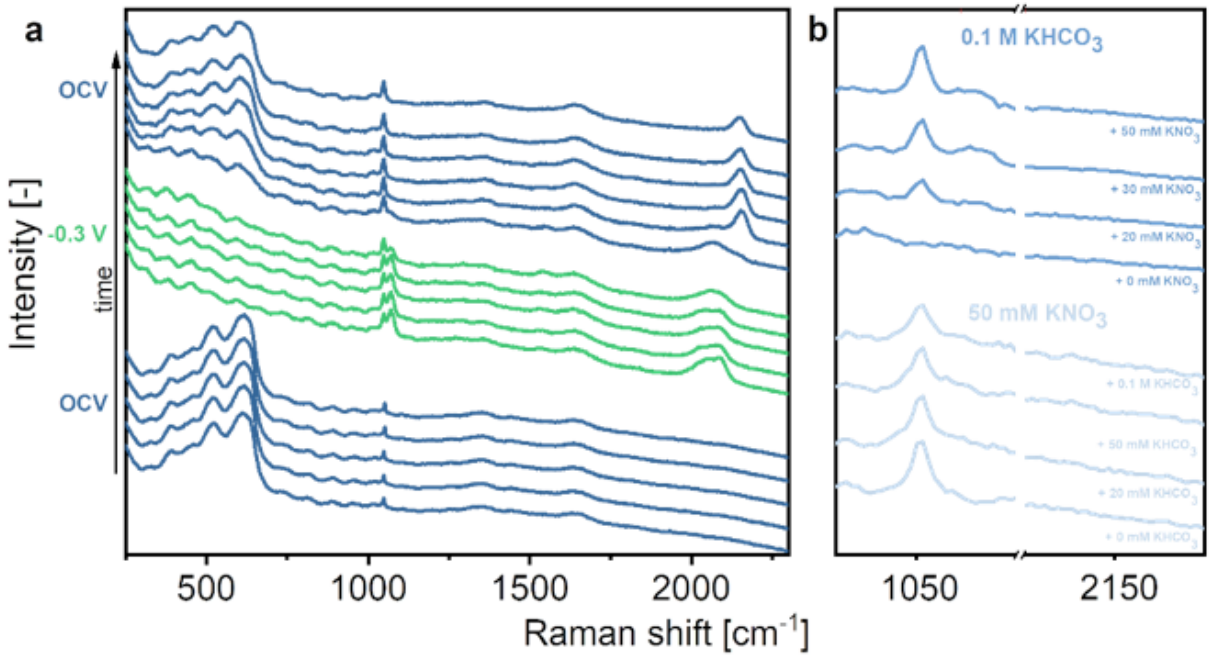

Figure 2

In situ SERS of a Cu surface at open circuit voltage. (a) CO2 saturated 0.1 M KHCO3 with 50 mM KNO3 electrolyte recorded at OCV, at -0.3 V vs RHE and again at OCV (the time interval between spectra is 1 min). (b) SERS spectra recorded at OCV after cyclic voltammetry in CO2 saturated 0.1 M KHCO3 (dark blue) or Ar/CO2 saturated 50 mM KNO3 (light blue) with addition of different amounts of KHCO3 or KNO3 at OCV.

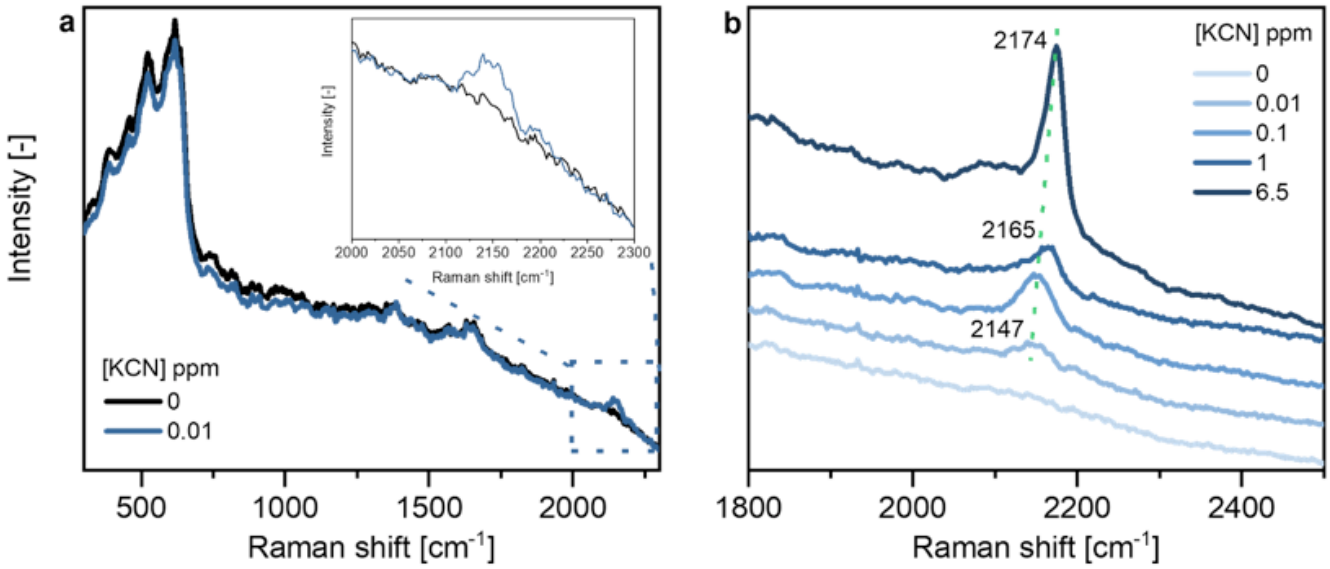

Figure 3

In situ SERS of a Cu surface in CO2 saturated 0.1 M KHCO3 at OCV with addition of KCN. (a) With 0 and 0.01 ppm of KCN; (b) with increasing concentration of KCN.

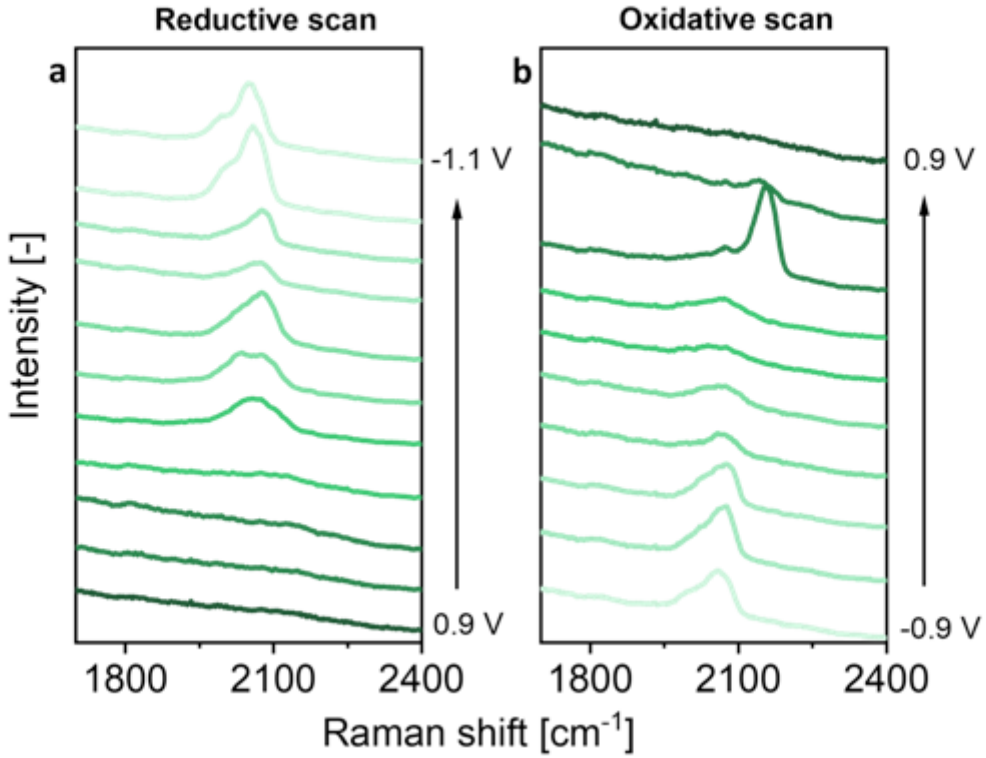

Figure 4

In situ SERS during cyclic Voltametry of a Cu surface in CO2 saturated 0.1 M KHCO3 with 0.1 ppm KCN. Recorded during (a) a reductive scan and (b) an oxidative scan.

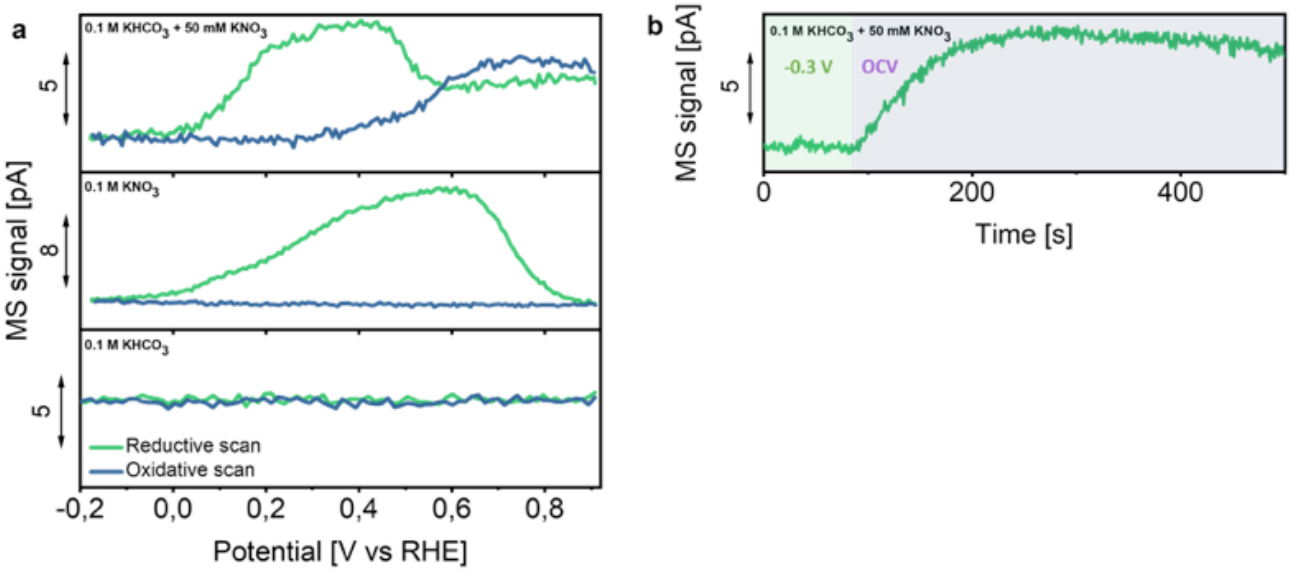

Figure 5

MS analysis of nitric oxide (m/z: 30) desorbed from the Cu surface. (a) During cyclic voltammetry (second cycle) in different electrolytes. (b) During chronoamperometry at -0.3 V vs RHE (green domain) and subsequent OCV (violet domain) in CO2 saturated 0.1 M KHCO3 + 50 mM KNO3.

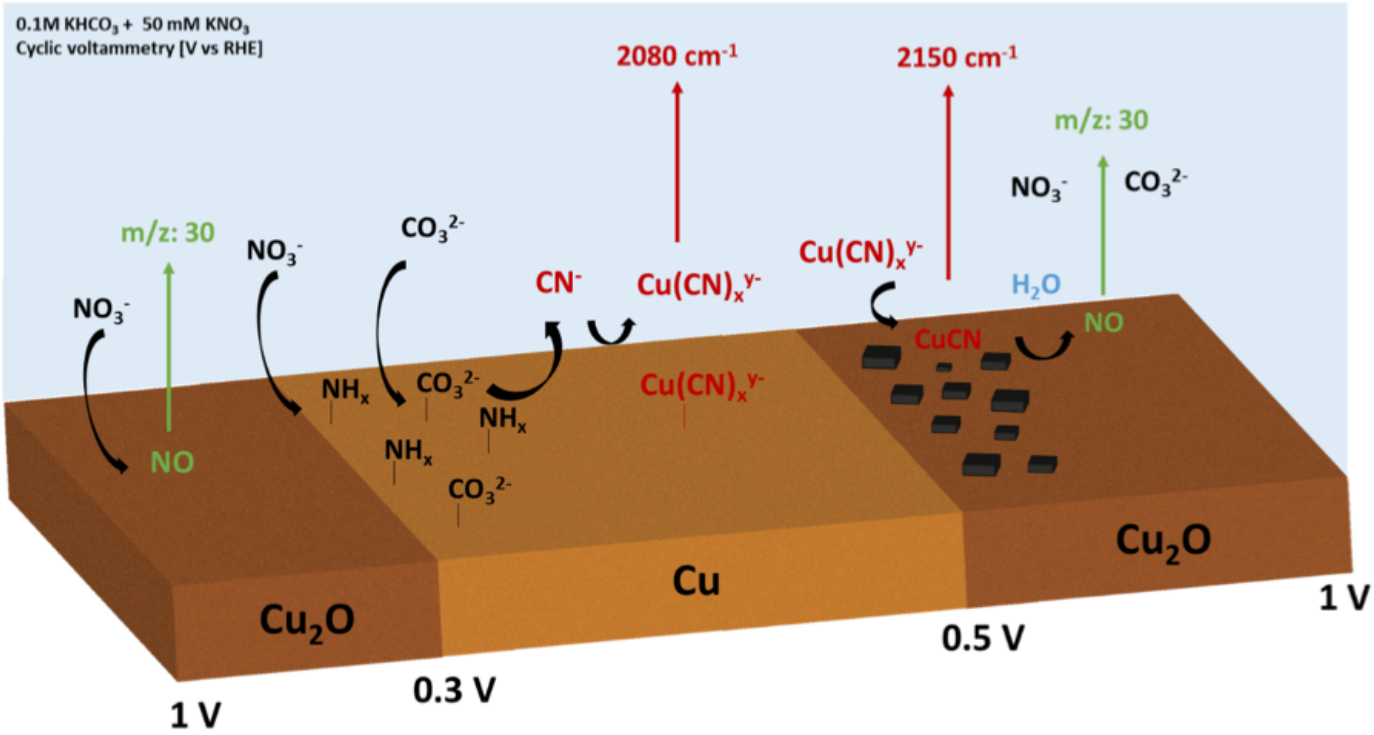

Figure 6

Summary scheme of CO2 electroreduction in the presence of NO3-, evaluated by SERS and EC-MS. Presented as one cyclic voltammetry cycle.

Supplementary Files

This is a list of supplementary files associated with this preprint. Click to download.

- CuCNbondformationSIPiotrv5GM.docx
- floatimage1.png